Dalton
Transactions

This article can be cited before page numbers have been issued, to do this please use: A. Doddi, D. Bockfeld, M. Zaretzke, C. Kleeberg, T. Bannenberg and M. Tamm, *Dalton Trans.*, 2017, DOI: 10.1039/C7DT03436A.

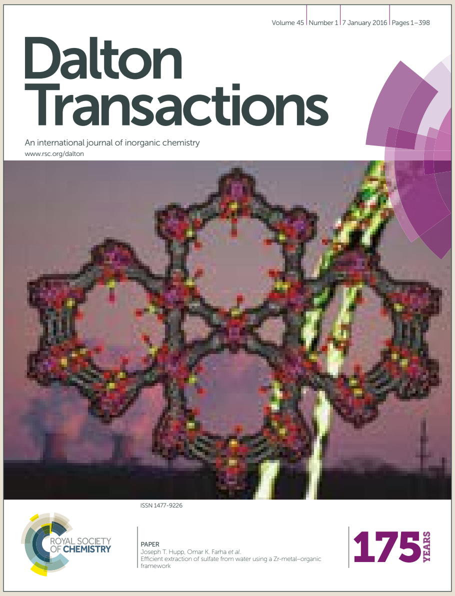

Volume 45 | Number 1 | 7 January 2016 | Pages 1–398

Dalton
Transactions

An international journal of inorganic chemistry
www.rsc.org/dalton

ISSN 1477-9226

ROYAL SOCIETY OF CHEMISTRY

PAPER
Joseph T. Hupp, Omar K. Farha et al.
Efficient extraction of sulfate from water using a Zr-metal-organic framework

175 YEARS

View Article Online
DOI: 10.1039/C7DT03436A

Journal Name

ARTICLE

A Modular Approach to Carbene-Stabilized Diphosphorus Species

Adinarayana Doddi, Dirk Bockfeld, Marc-Kevin Zaretzke, Christian Kleeberg, Thomas Bannenberg and Matthias Tamm*

Received 00th January 20xx,
Accepted 00th January 20xx

DOI: 10.1039/x0xx00000x

www.rsc.org/

Heteroleptic N-heterocyclic dicarbene-diphosphorus species were prepared by reaction of the carbene-phosphinidene adduct (IPr)PSiMe$_3$ (**1**, IPr = 1,3-bis(2,6-diisopropylphenyl)imidazolin-2-ylidene) with the carbene-phosphorus trichloride adduct (IMes)PCl$_3$ (**2**, IMes = 1,3-bis(2,4,6-trimethylphenyl)imidazolin-2-ylidene), which furnished the dichloride [(IPr)PPCl(IMes)]Cl (**3**). Reduction of **3** with potassium graphite (KC$_8$) afforded [(IPr)PP(IMes)] (**4**). The corresponding radical cation [(IPr)PP(IMes)]$^{+\cdot}$ (**5**$^{+\cdot}$) is isolated as [**5**]PF$_6$ by reaction of **4** with ferrocenium hexafluorophosphate, whereas complexes containing the corresponding dication [(IPr)PP(IMes)]$^{2+}$ (**6**$^{2+}$) can be isolated as the gallate and borate salts [**6**](GaCl$_4$)$_2$ and [**6**](BAr^F)$_2$ by chloride abstraction from **3** with GaCl$_3$ or sodium tetrakis[bis(3,5-trifluoromethyl)phenyl]-borate (NaBAr^F), respectively. The asymmetric set of N-heterocyclic carbene ligands allows to establish $^1J_{PP}$ coupling constants of 249 Hz for **4** and 543 Hz for [**6**](GaCl$_4$)$_2$. Based on X-ray diffraction analyses, the molecular stuctures of **4**, **5**$^{+\cdot}$ and **6**$^{2+}$ reveal a consecutive shortening of the P–P bond lengths, in agreement with the presence of a phosphorus-phosphorus single bond in **4** and a double bond in **6**$^{2+}$, which is best described as a dicationic diphosphene according to density functional theory (DFT) calculations.

Introduction

The preparation of carbene-stabilized "main-group diatomic allotropes"[1] has been one of the most remarkable achievements in the application of N-heterocyclic carbenes (NHC) in main-group element chemistry.[2] For group 15, this development commenced with the isolation of "carbene-stabilized diphosphorus" in the homoleptic dicarbene complexes [(IPr)$_2$P$_2$] (**A**) and [(IMes)$_2$P$_2$] (**B**),[3] although it should be noted that acyclic diphosphorus compounds of the type [{(R$_2$N)$_2$C}$_2$P$_2$] (R = Me, Et) have been known since 1985.[4] P$_2$-stabilization with a cyclic alkyl amino carbene (CAAC) in **C** was also achieved (Chart 1),[5] and shortly after, stepwise oxidation of **A** and **C** to carbene-stabilized P$_2$-radical cations and P$_2$-dications was reported.[6] A similar series [(IPr)$_2$As$_2$]$^{0,+\cdot,2+}$ was isolated from the diarsenic congener of **A**,[7] and a diatomic antimony analogue of **C** was also prepared.[8] All NHC complexes mentioned above were prepared by reduction of a single precursor of the type (NHC)ECl$_3$, which affords homoleptic dicarbene-dielement complexes. It appeared desirable to provide routes to related heteroleptic dielement species like **4** with two different NHC ligands, since important spectroscopic data such as ^{31}P-^{31}P coupling constants could be derived. Moreover, a general modular approach would also allow to access compounds with an asymmetric dielement moiety EE' (E ≠ E', e.g., EE' = PAs), and the use of different NHC ligands could help to avoid crystallographic disorder problems. Rare examples in which an EE' moiety is flanked by two different carbenes are represented by "carbene-stabilized phosphorus mononitride" **D** and its corresponding radical cation.[9]

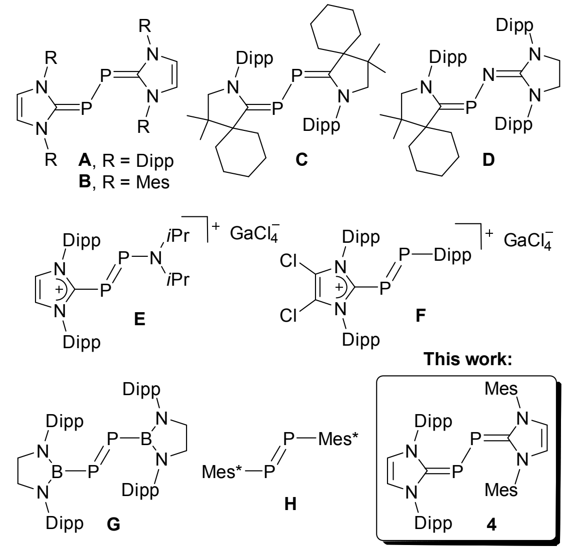

Chart 1 A few examples of neutral and cationic main-group element-element species stabilized by sterically bulky substituents (Dipp = 2,6-diisopropylphenyl, Mes = 2,4,6-trimethylphenyl, Mes* = 2,4,6-tri-*tert*-butylphenyl).

To the best of our knowledge, only a few asymmetric P$_2$ systems containing NHC ligands are known, namely the cation-

---

[a] Institut für Anorganische und Analytische Chemie, Technische Universität Braunschweig, Hagenring 30, 38106 Braunschweig, Germany;
E-mail: m.tamm@tu-bs.de.

† Electronic Supplementary Information (ESI) available: NMR spectra, crystallographic and computational details. CCDC reference numbers 1572769–1572775. See DOI: 10.1039/x0xx00000x

View Article Online
DOI: 10.1039/C7DT03436A

ic monocarbene complexes **D** and **E**, which were isolated and structurally characterized as their tetrachlorogallate salts (Chart 1).[10,11] These compounds are best described as cationic diphosphenes and were shown to undergo cycloaddition reactions along the polarized phosphorus-phosphorus double bond.[10,12] Related monocarbene species [(IPr)SiP(Mes*)] and [(CAAC)PSiX] (X = benzamidinate) containing isoelectronic Si=P moieties were also reported.[13] The boryl-substituted diphosphene **G** represents another interesting system,[14] which is isolelectronic to the dication $[(\text{IPr})_2\text{P}_2]^{2+}$ obtained by two-electron oxidation from **A**. Clearly, the latter system as well as compounds **E**–**G** are closely related to conventional diphosphenes,[15] e.g., Yoshifuji's iconic bis(2,4,6-tri-*tert*-butylphenyl)-diphosphene (**H**).[16] In this contribution, we present the synthesis of heteroleptic $[(\text{IPr})\text{P}_2(\text{IMes})]$ (**4**) and its oxidation to the corresponding radical cation $[(\text{IPr})\text{P}_2(\text{IMes})]^{+\cdot}$ ($\mathbf{5}^{+\cdot}$) and dication $[(\text{IPr})\text{P}_2(\text{IMes})]^{2+}$ ($\mathbf{6}^{2+}$) by using a modular approach based on the N-heterocyclic carbene-phosphinidene adduct $(\text{IPr})\text{PSiMe}_3$ (**1**), which we have developed previously for the preparation of NHC-phosphinidenide transition metal complexes of the type $[(\text{NHC})\text{PML}_n]$.[17,18]

Results and discussion

The reaction of **1** with the carbene adduct of phosphorus trichloride $(\text{IMes})\text{PCl}_3$ (**2**)[3] in toluene at elevated temperature furnished a yellow-orange crystalline solid of the composition [(IPr)P(Cl)P(IMes)]Cl (**3**), as indicated by high-resolution mass spectrometry and elemental analysis (Scheme 1). The ^{31}P NMR spectrum in CD_2Cl_2 reveals the formation of two isomers in approx. 4:1 ratio, which both give rise to two doublets with distinctly different chemical shifts at 138.3 and –21.8 ppm ($^1J_{\text{PP}}$ = 381 Hz) for the major compound and at 128.4 and –28.3 ppm ($^1J_{\text{PP}}$ = 373 Hz) for the minor compound, indicating a downfield shift for one of the ^{31}P nuclei due to the presence of a phosphorus-chlorine bond. Similar values were reported for the related cationic chlorine- and bromine-containing species [(IPr)PPCl(IPr)]OTf (δ = 132.1, –22.4 ppm, $^1J_{\text{PP}}$ = 388 Hz)[19] and $[(\text{IPr})\text{PPBr}(\text{IPr})][\text{SnBr}_5(\text{THF})]$ (δ = 145.4, –7.6 ppm, $^1J_{\text{PP}}$ = 391 Hz),[20] whereas a smaller coupling constant was found for protonated **A**, *i.e.* [(IPr)PPH(IPr)]Cl (δ = –105.2, –109.8 ppm, $^1J_{\text{PP}}$ = 235 Hz).[21]

Single-crystals of **3**·3 CH_2Cl_2 were grown from dichloromethane solution at –30 °C, and X-ray diffraction analysis revealed the formation of the cation $[(\text{IPr})\text{PPCl}(\text{IMes})]^+$, in which the chlorine atom is bound to the phosphorus atom (P2–Cl1 = 2.1560(11) Å) that bears the sterically less demanding IMes ligand (Figure 1). The chloride counterion is well separated with the shortest P–Cl2 distance of 7.1679(11) Å and displays several short C–H···Cl contacts to the CH_2Cl_2 solvate molecules and to the NHC backbones. The P1–P2 bond length is 2.1067(10) Å, which is very similar compared to the cation $[(\text{IPr})\text{PPBr}(\text{IPr})]^+$ (P1–P2 = 2.096(2) Å) for the structure with a $[\text{SnBr}_6]^{2-}$ counterion,[20] and to [(IPr)PPH(IPr)]Cl (2.098(13) Å).[21] DFT calculations at the B97-D/6-311G(d,p) level of theory reveal very similar Gibbs free energies (ΔG_{298} = 2.6 kcal mol^{-1}) for the cation $[(\text{IPr})\text{PPCl}(\text{IMes})]^+$ as observed in the solid-state and for the isomeric cation $[(\text{IMes})\text{PPCl}(\text{IPr})]^+$, in which the chlorine atom is bound to the phosphorus atom flanked by the IPr ligand (ESI†). Consequently, an unambiguous assignment of the NMR signals of the major and minor compounds present in solution to these two isomers cannot be made.

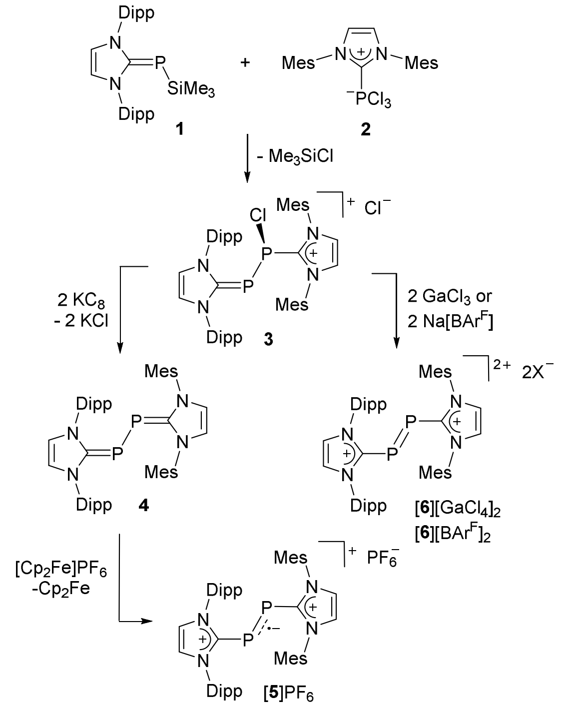

Scheme 1 Synthesis of heteroleptic dicarbene-diphosphorus compounds; $[\text{BAr}^{\text{F}}]^-$ indicates the tetrakis[bis(3,5-trifluoromethyl)phenyl]borate counterion.

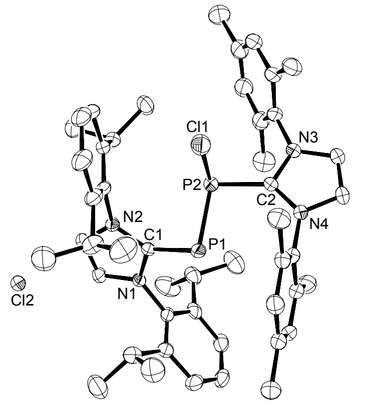

Fig. 1 ORTEP diagrams of **3** in **3**·3CH_2Cl_2 with thermal displacement parameters drawn at 50% probability level; hydrogen atoms and solvent molecules are omitted for clarity. Selected bond lengths [Å] and angles [°]: P1–P2 2.1067(10), P2–Cl1 2.1560(11), P1–C1 1.817(3), P2–C2 1.851(3); C1-P1-P2 94.99(9), C2-P2-P1 99.89(9), P1–P2–Cl1 113.14(5), C2–P2–Cl1 93.75(9).

It should be noted that compound **3** can be formally regarded as either a P(I)-P(I) dimer or a mixed valence species with the phosphorus atom in the +2 and 0 oxidation states.[20] Whatever case might be more appropriate, two-electron reduction of **3** should furnish the heteroleptic dicarbene-

View Article Online
DOI: 10.1039/C7DT03436A

diphosphorus(0) compound **4**. Indeed, this compound was isolated as a dark red solid in 84% yield by reaction of **3** with potassium graphite (KC_8) in THF solution (Scheme 1). The ^1H NMR spectrum shows the signals expected for the IPr and IMes carbene ligands, and for instance, the imidazole CH resonances are 5.99 (IPr) and 5.74 (IMes) ppm, which perfectly matches the values reported for the homoleptic congeners $(IPr)_2P_2$ (**A**, 5.98 ppm) and $(IMes)_2P_2$ (**B**, 5.71 ppm).[3] Whereas the latter give rise to ^{31}P NMR singlet resonances at –52.4 and –73.6 ppm, the ^{31}P NMR spectrum of **4** exhibits a higher-order AB spin system because of the presence of two magnetically different phosphorus nuclei (Figure 2, left). The two doublets are centered at –63.1 and –59.4 ppm with $^1J_{PP}$ = 249 Hz; this ^{31}P–^{31}P coupling constant is significantly smaller than those of **3** (381 Hz and 373 Hz) and related compounds, in agreement with a reduced bond order and the presence of a P–P single bond.

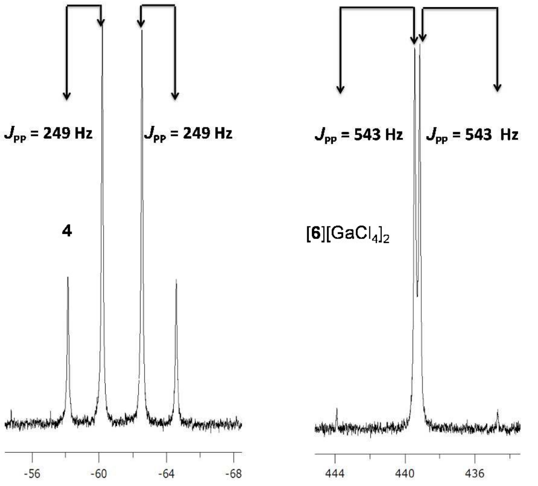

Fig. 2 ^{31}P NMR spectra of **4** (left, in C_6D_6) and [**6**]$[GaCl_4]_2$ (right, in CD_2Cl_2).

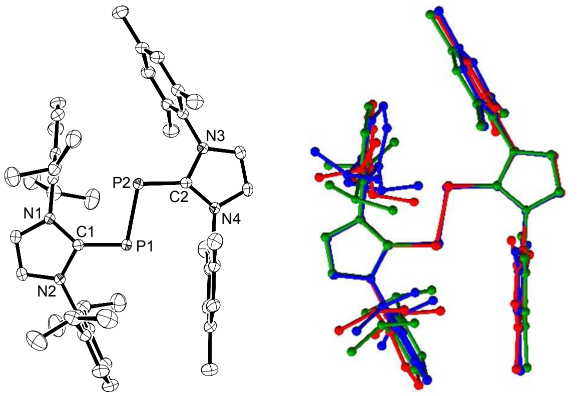

Fig. 3 Left: ORTEP diagram of **4** with thermal displacement parameters drawn at 50 % probability level; hydrogen atoms are omitted for clarity. **Right:** Overlay of the molecular structures of **4** (red) and of the mono- and dications in **5**$^{+\cdot}$ in [**5**]$PF_6{\cdot}2CH_2Cl_2$ (green) and **6**$^{2+}$ in [**6**]$[GaCl_4]_2$ (blue). Pertinent structural data are assembled in Table 1. Selected torsion angles [°] in **4**/**5**$^{+\cdot}$/**6**$^{2+}$: C1–P1–P2–C2 163.07(6)/176.1(1)/178.1(1), N1–C1–P1–P2 1.83(12)/12.0(2)/ 6.6(3), N4–C4–P2–P1 8.49(13)/6.0(3)/3.7(3).

This assignment was confirmed by X-ray diffraction analysis, and the molecular structure of **4** reveals a P1–P2 bond length of 2.1897(4) Å (Figure 3, left), which is almost identical with the values established for homoleptic **A** (2.2052(10) Å) and **B** (2.1897 (11) Å)[3] and also falls in the range of the phosphorus-phosphorus distances in elemental P_4 (2.21 Å).[22] The $P–C_{carbene}$ bond lengths of 1.7502(11) (P1–C1) and 1.7488(11) Å (P2–C4) are also very similar compared to **A** and **B**; they are slightly shorter than the polarized P–C double bonds in typical N-heterocyclic carbene-phosphinidene adducts, e.g., 1.7658(10) Å in (IPr)PPh and 1.763(6) Å in (IMes)PPh.[23] **4** also shows the typical *trans*-bent geometry and a slightly twisted, but nearly coplanar orientation of the imidazole rings towards the central P–P bond as indicated by torsion angles of 163.1° (C1–P1–P2–C4), 1.8° (N1–C1–P1–P2), and 8.5° (N4–C4–P2–P1). It should be noted that our modular approach proved also useful for the preparation of the symmetric dicarbene-diphosphorus species **A**,[3] and the reaction of **1** with $(IPr)PCl_3$ furnished [(IPr)PPCl(IPr)]Cl, which was reduced with KC_8 in THF to give **A** in 88% yield after a very simple work-up procedure (ESI†).

It was previously demonstrated that oxidation of $[(IPr)_2P_2]$ (**A**) with the trityl borate $(Ph_3C)[B(C_6F_5)_4]$ or with ferrocenium trifluoromethanesulfonate, Fc(OTf), affords the corresponding carbene-stabilized P_2-radical cation and P_2-dications $[(IPr)_2P_2]^{+\cdot}$ and $[(IPr)_2P_2]^{2+}$, respectively.[6] In principle, the cyclic voltammogram of **4** is like that of **A** and shows two quasireversible oxidations, the first at $E_{1/2}$= –1.55 V and the second at $E_{1/2}$= –0.51 V *vs.* the ferrocene/ferrocenium (Fc/Fc$^+$) couple (THF solution, 0.1 M *n*-Bu_4NPF_6 as electrolyte, Figure S20, ESI†). Accordingly, treatment of **4** with one eq. of $[Fc]PF_6$ in THF afforded the novel carbene-stabilized main group radical species $[(IPr)PP(IMes)]PF_6$, [**5**]PF_6, as a dark green solid (Scheme 1).[24] The X-band EPR spectrum of a CH_2Cl_2 solution at room temperature is shown in Figure 4 (left); it exhibits a triplet with an isotropic *g* value of 2.00865 and a hyperfine coupling constant to the two phosphorus nuclei of $A(^{31}P)$ = 43.4 G, which is almost identical with the value reported for homoleptic $[(IPr)_2P_2][B(C_6F_5)_4]$ ($A(^{31}P)$ = 43 G). Moreover, hyperfine coupling with the four ^{14}N nuclei is also resolved ($A(^{14}N)$ = 1.6 G). In line with these results, the calculated spin density in **5**$^{+\cdot}$ is largely distributed between the two phosphorus atoms (0.32*e* and 0.36*e*) with additional small localization on the four nitrogen atoms (0.04*e*–0.05*e*, Figure 4, right).

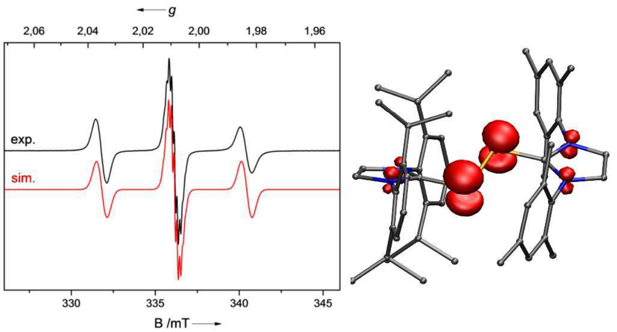

View Article Online
DOI: 10.1039/C7DT03436A

Fig. 4 Left: Experimental (black) and simulated (red) X-band EPR spectrum of [**5**]PF_6 in CH_2Cl_2 (298 K, 9.450643 GHz). **Right**: Spin density distribution of radical **5**$^{+\cdot}$.

Table 1 Comparison of selected experimental and calculated bond lengths and associated Wiberg Bond Indices (WBI) and Relaxed Force Constants (RFC)[a]

Comp.	P–P			P–C_{IPr}			P–C_{IMes}		
	d (Å)[b]	WBI	RFC (N cm^{-1})	d (Å)[b]	WBI	RFC (N cm^{-1})	d (Å)[b]	WBI	RFC (N cm^{-1})
4	2.231/ 2.1897(4)	1.03	1.51	1.769/ 1.7502(11)	1.35	3.31	1.768/ 1.7488(11)	1.33	3.30
5$^{+\cdot}$	2.159/ 2.1088(7)[c]	1.23	2.02	1.817/ 1.806(2)	1.08	2.62	1.805/ 1.797(2)	1.12	2.77
6^{2+}	2.081/ 2.0450(11)[d]	1.67	2.65	1.844/ 1.816(3)	0.95	2.48	1.830/ 1.822(3)	1.01	2.55

[a] DFT B97-D/6-311G(d,p). [b] Theoretical/experimental bond lengths. [c] P–P bond lengths in [**5**]PF_6·$2CH_2Cl_2$. [d] P–P bond length in [**6**][$GaCl_4$]$_2$.

Further oxidation of **5**$^{+\cdot}$, or two-electron oxidation of **4**, should furnish the dication [(IPr)PP(IMes)]$^{2+}$ (**6**$^{2+}$); however, this system is also conveniently accessible directly from **3** by abstraction of the two chloride ions. This reaction can be accomplished by addition of two equivalents of $GaCl_3$ in dichlormethane to form [(IPr)PP(IMes)][$GaCl_4$]$_2$, [**6**][$GaCl_4$]$_2$, as an orange crystalline solid in 65% yield (Scheme 1). Alternatively, the borate salt [(IPr)PP(IMes)][BAr^F]$_2$ can be isolated in 79% yield by addition of sodium tetrakis[bis(3,5-trifluoromethyl)-phenyl]borate (NaBAr^F). This compound was also fully characterized, affording similar spectroscopic and structural features (ESI†). The following discussion will be restricted to the tetrachlorogallate salt [**6**][$GaCl_4$]$_2$. Its ^{31}P NMR spectrum shows again a higher-order AB spin system with even stronger roofing (Figure 2, right); the corresponding doublets are observed at significantly lower field at 438.5 and 440.1 ppm with $^1J_{PP}$ = 543 Hz. These chemical shifts fall in the range reported for diphosphenes such as **H** (δ = 492.4 ppm)[25] and also for the closely related homoleptic dicarbene-diphosphorus system [$(IPr)_2P_2$](OTf)$_2$ (δ = 452 ppm),[6] whereas the boryl-substituted diphosphene **G** exhibits a resonance at significantly lower field (605 ppm). The ^{31}P–^{31}P coupling constant is similar to the values determined for asymmetric diphosphenes of the type RPPR′,[15] and the ^{31}P NMR spectra of the related monocationic diphosphenes **D** and **E** exhibit AX spin systems with $^1J_{PP}$ couplings of 578 and 525 Hz, respectively.[10,11] A much larger coupling constant of 884 Hz was reported for a singlet phosphinidene [{CH_2NAr^*}$_2$PP] (Ar* = 2,6-dibenzhydryl-4-methylphenyl), for which a bond order >2 was discussed.[26]

The molecular structures of [**5**]PF_6·$2CH_2Cl_2$ and [**6**][$GaCl_4$]$_2$ could be established by X-ray diffraction analyses;[27] ORTEP diagrams can be found in the ESI section (Figures S42 and S45). Figure 3 (right) shows an overlay of the structures of **4**, **5**$^{+\cdot}$, and **6**$^{2+}$, revealing that the *trans*-bent geometry and coplanar arrangement in **4** is retained in the oxidized cationic species with relevant torsion angles (C1–P1–P2–C2, N1–C1–P1–P2, N4–C4–P2–P1) close to 180° or 0°, respectively. In contrast, significantly more twisted structures were found for the homoleptic analogues [$(IPr)_2P_2$]$^{+\cdot}$ and [$(IPr)_2P_2$]$^{2+}$, with the latter showing a perpendicular orientation of the imidazole planes towards the central P–P bond,[6] an arrangement that is also prevalent in diaryldiphosphenes such as **H**.[28–30] Upon oxidation, the P1–P2 bond shortens from 2.1897(4) Å in **4** to 2.1088(7) Å in **5**$^{+\cdot}$ and 2.0450(11) Å in **6**$^{2+}$, whereas a consecutive elongation of the P–$C_{carbene}$ bonds is observed (Table 1). The P1–P2 bond length in **5**$^{+\cdot}$ is virtually identical with the value reported for [$(IPr)_2P_2$][BAr^F] (2.111(1) Å),[20] while this bond length in **6**$^{2+}$ is similar to the P–P distances in typical diphosphenes,[15,28,29] e.g., 2.034(2)/2.046(2) Å for two independent X-ray crystal determinations of **H**.[16,31] Likewise, the P–P bond lengths in **D** (2.038(1) Å),[11] **E** (2.0611(7) Å),[10] **G** (2.0655(17) Å),[14] and [$(IPr)_2P_2$](OTf)$_2$ (2.0826(12) Å)[6] fall in a similar range.

To assess the bonding situation further in the diphosphorus species **4**, **5**$^{+\cdot}$ and **6**$^{2+}$, their structures were optimized applying the density functional theory (DFT) method B97-D, followed by natural bond orbital (NBO) analysis. The computational details are described in Chapter D (ESI†), and contour plots of selected NBOs are shown in Tables S9–S11. Overall, the computed structural parameters are in sufficient agreement with those determined in the solid state, although consistently longer P–P and P–$C_{carbene}$ bond lengths were found (Table 1). Nevertheless, the trend for these bond lengths upon oxidation is accurately reproduced, with consecutive shortening of the P–P bonds and concurrent elongation of the P–$C_{carbene}$ bonds in the series **4**, **5**$^{+\cdot}$ and **6**$^{2+}$. Accordingly, the trend of the Wiberg bond index (WBI) from 1.03 (**4**) to 1.23 (**5**$^{+\cdot}$) and 1.67 (**6**$^{2+}$) indicates an increase of the phosphorus-phosphorus bond order from a P–P single bond in **4** towards a P–P double bond in **6**$^{2+}$. Likewise, the trend of the corresponding P–$C_{carbene}$ WBI values reveals a consecutive weakening of these bonds (Table 1). Thereby, the Wiberg bond indices of 1.35 (P–C_{IPr}) and 1.33 (P–C_{IMes}) in **4** are in the range of those calculated for the polarized phosphorus-carbon double bonds in N-heterocyclic carbene-phosphinidene adducts such as (IPr)PH (1.37).[18] As an additional bond strength descriptor, we calculated relaxed force constants (RFC),[32] confirming the strengthening of the P–P bond upon oxidation. An analogous conclusion was drawn for the homoleptic series [$(IPr)_2P_2$]$^{0/+\cdot/2+}$ based on the increase of the P–P bond dissociation energies (D_e).[6]

View Article Online
DOI: 10.1039/C7DT03436A

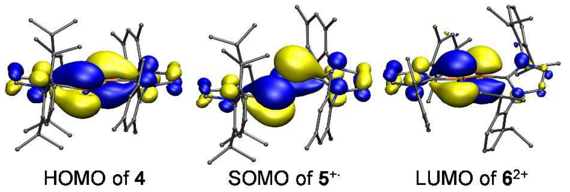

Fig. 5 Frontier molecular orbitals in **4**, $\mathbf{5}^{+\cdot}$ and $\mathbf{6}^{2+}$ with mainly π*(P–P) character.

Similarly, these findings can be rationalized by analysis of the frontier molecular orbitals in **4**, $\mathbf{5}^{+\cdot}$ and $\mathbf{6}^{2+}$ (Figure 5), which reveals that the highest occupied molecular orbital (HOMO) in **4** is mainly π*(P–P) antibonding in character with a significant π(P–$C_{carbene}$) binding contribution. Therefore, successive removal of electrons from this orbital, which affords the corresponding singly occupied molecular orbital (SOMO) in $\mathbf{5}^{+\cdot}$ and the lowest unoccupied molecular orbital (LUMO) in $\mathbf{6}^{2+}$, allows to explain the observed progression of the bond lengths and strengths unequivocally.

Conclusions

We have presented a modular approach for the preparation of heteroleptic dicarbene-diphosphorus adducts of the type $[(IPr)PP(IMes)]^x$ (**4**, x = 0; **5**, x = +·; **6**, x = 2+), which allows to establish phosphorus-phosphorus coupling constants for the diamagnetic neutral and dicationic species as an additional experimental parameter for the characterization of the P–P bonding situation. The experimental and theoretical findings agree with the presence of single and double bonds in **4** and $\mathbf{6}^{2+}$, with the latter best described as a dicationic diphosphene. As expected, the radical cation $\mathbf{5}^{+\cdot}$ adopts an intermediate position with a singly-occupied antibonding π*(P–P) molecular orbital. Moreover, we are convinced that our modular approach will allow to construct hetero-dielement compounds, e.g., with a phosphorus-arsenic bond by combination of carbene-phosphinidene or carbene-arsinidene adducts (NHC)$ESiMe_3$ (E = P, As)[33] with carbene adducts of phosphorus or arsenic trichlorides (NHC')$E'Cl_3$ (E' = P, As), and we hope to report the isolation of these and related species in due course.

Conflicts of interest

There are no conflicts to declare.

Acknowledgements

Financial support from the Deutsche Forschungsgemeinschaft (DFG) through grant TA 189/16-1 (N-Heterocyclic Phosphinidyne Ligands) is gratefully acknowledged.

Notes and references

References

1 (*a*) Y. Wang and G. H. Robinson, *Dalton Trans.*, 2012, **41**, 337–345; (*b*) D. J. D. Wilson and J. L. Dutton, *Chem. Eur. J.*, 2013, **19**, 13626–13637;

2 (*a*) D. Bourissou, O. Guerret, F. P. Gabbaï and G. Bertrand, *Chem. Rev.*, 2000, **100**, 39–92; (*b*) N. Kuhn and A. Al-Sheikh, *Coord. Chem. Rev*, 2005, **249**, 829–857; (*c*) Y. Wang and G. H. Robinson, *Inorg. Chem.*, 2011, **50**, 12326–12337; (*d*) M. N. Hopkinson, C. Richter, M. Schedler and F. Glorius, *Nature*, 2014, **510**, 485–496; (*e*) Y. Wang and G. H. Robinson, *Inorg. Chem.*, 2014, **53**, 11815–11832;

3 Y. Wang, Y. Xie, P. Wei, R. B. King, H. F. Schaefer III, P. v. R. Schleyer and G. H. Robinson, *J. Am. Chem. Soc.*, 2008, **130**, 14970–14971.

4 V. D. Romanenko, L. S. Kachkovskaya, L. N. Markovskii, *Zh. Obshch. Khim.*, 1985, **55**, 2140 – 2141.

5 O. Back, G. Kuchenbeiser, B. Donnadieu and G. Bertrand, *Angew. Chem. Int. Ed.*, 2009, **48**, 5530–5533.

6 O. Back, B. Donnadieu, P. Parameswaran, G. Frenking and G. Bertrand, *Nat. Chem.*, 2010, **2**, 369–373.

7 (*a*) M. Y. Abraham, Y. Wang, Y. Xie, P. Wei, H. F. Schaefer III, P. v. R. Schleyer and G. H. Robinson, *Chem. Eur. J.*, 2010, **16**, 432–435; (*b*) M. Y. Abraham, Y. Wang, Y. Xie, R. J. Gilliard Jr., P. Wei, B. J. Vaccaro, M. K. Johnson, H. F. Schaefer III, P. v. R. Schleyer and G. H. Robinson, *J. Am. Chem. Soc.*, 2013, **135**, 2486–2488;

8 R. Kretschmer, D. A. Ruiz, C. E. Moore, A. L. Rheingold and G. Bertrand, *Angew. Chem. Int. Ed.*, 2014, **53**, 8176–8179.

9 R. Kinjo, B. Donnadieu and G. Bertrand, *Angew. Chem. Int. Ed.*, 2010, **49**, 5930–5933.

10 A. Beil, R. J. Gilliard Jr. and H. Grützmacher, *Dalton Trans.*, 2016, **45**, 2044–2052.

11 K. Schwedtmann, M. H. Holthausen, C. H. Sala, F. Hennersdorf, R. Fröhlich and J. J. Weigand, *Chem. Commun.*, 2016, **52**, 1409–1412.

12 K. Schwedtmann, F. Hennersdorf, A. Bauzá, A. Frontera, R. Fischer and J. J. Weigand, *Angew. Chem. Int. Ed.*, 2017, **100**, 2494.

13 (*a*) D. Geiß, M. I. Arz, M. Straßmann, G. Schnakenburg and A. C. Filippou, *Angew. Chem. Int. Ed.*, 2015, **54**, 2739–2744; (*b*) S. Kundu, B. Li, J. Kretsch, R. Herbst-Irmer, D. M. Andrada, G. Frenking, D. Stalke and H. W. Roesky, *Angew. Chem. Int. Ed.*, 2017, **56**, 4219–4223;

14 S.-s. Asami, M. Okamoto, K. Suzuki and M. Yamashita, *Angew. Chem. Int. Ed.*, 2016, **55**, 12827–12831.

15 L. Weber, *Chem. Rev*, 1992, **92**, 1839–1906.

16 M. Yoshifuji, I. Shima, N. Inamoto, *J. Am. Chem. Soc.*, 1981, **103**, 4587–4589.

17 A. Doddi, D. Bockfeld, T. Bannenberg, P. G. Jones and M. Tamm, *Angew. Chem. Int. Ed.*, 2014, **53**, 13568–13572.

18 M. Peters, A. Doddi, T. Bannenberg, M. Freytag, P. G. Jones and M. Tamm, *Inorg. Chem.*, 2017, **56**, 10785–10793.

View Article Online
DOI: 10.1039/C7DT03436A

19 F. D. Henne, E.-M. Schnöckelborg, K.-O. Feldmann, J. Grunenberg, R. Wolf and J. J. Weigand, *Organometallics*, 2013, **32**, 6674–6680.

20 J. B. Waters, T. A. Everitt, W. K. Myers and J. M. Goicoechea, *Chem. Sci.*, 2016, **7**, 6981–6987.

21 Y. Wang, H. P. Hickox, Y. Xie, P. Wei, D. Cui, M. R. Walter, H. F. Schaefer III and G. H. Robinson, *Chem. Commun.*, 2016, **52**, 5746–5748.

22 I. Krossing, *J. Am. Chem. Soc.*, 2001, **123**, 4603–4604.

23 (*a*) A. Doddi, D. Bockfeld, A. Nasr, T. Bannenberg, P. G. Jones and M. Tamm, *Chem. Eur. J.*, 2015, **21**, 16178–16189; (*b*) A. J. Arduengo III, J. C. Calabrese, A. H. Cowley, Dias, H. V. R., J. R. Goerlich, W. J. Marshall and B. Riegel, *Inorg. Chem.*, 1997, **36**, 2151–2158;

24 C. D. Martin, M. Soleilhavoup and G. Bertrand, *Chem. Sci.*, 2013, **4**, 3020–3030.

25 M. Yoshifuji, I. Shima, N. Inamoto, K. Hirotsu and T. Higuchi, *J. Am. Chem. Soc.*, 1982, **104**, 6167.

26 L. Liu, D. A. Ruiz, D. Munz and G. Bertrand, *Chem*, 2016, **1**, 147–153.

27 The structure of [**6**][BAr^F]$_2$ was also established, but it suffers from severe disorder of the P_2 moiety and several CF_3 groups and provides little more information than confirming the connectivity. Likewise, the [$GaCl_4$]$^-$ counterions in [**6**][$GaCl_4$]$_2$ show positional disorder. Both structures contain residual electron density that could not be modelled appropriately and was assigned to co-crystallized CH_2Cl_2. Therefore, the data were processed using the SQUEEZE/ PLATON program (A. L. Spek, *Acta Crystallogr., Sect. C: Struct. Chem.*, 2015, **71**, 9–18). For both compounds, several crystals from different batches exhibited the same crystallographic problems.

28 P. P. Power, *Chem. Rev.*, 1999, **99**, 3463–3504.

29 R. C. Fischer and P. P. Power, *Chem. Rev*, 2010, **110**, 3877–3923.

30 T. Sasamori and N. Tokitoh, *Dalton Trans.*, 2008, 1395–1408.

31 A. H. Cowley, A. Decken, N. C. Norman, C. Krüger, F. Lutz, H. Jacobsen and T. Ziegler, *J. Am. Chem. Soc.*, 1997, **119**, 3389–3390.

32 (*a*) K. Brandhorst and J. Grunenberg, *Chem. Soc. Rev.*, 2008, **37**, 1558–1567; (*b*) J. Grunenberg, *Chem. Sci.*, 2015, **6**, 4086–4088; (*c*) J. Grunenberg, *Int. J. Quantum Chem.*, 2017, **117**, e25359;

33 A. Doddi, M. Weinhart, A. Hinz, D. Bockfeld, J. M. Goicoechea, M. Scheer and M. Tamm, *Chem. Commun.*, 2017, **53**, 6069–6072.

View Article Online
DOI: 10.1039/C7DT03436A

TOC graphic

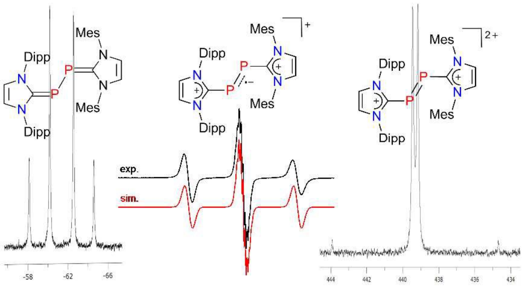

TOC text

A modular approach has been developed for the synthesis of a series of neutral, cationic and dicationic heteroleptic dicarbene-diphosphorus species.